ELSEVIER

Journal of Food Engineering 54 (2002) 45–58

JOURNAL OF FOOD ENGINEERING

www.elsevier.com/locate/jfoodeng

Heat transport to a starch slurry gelatinizing between the drums of a double drum dryer

M.A. Gavrielidou [a], N.A. Vallous [a], T.D. Karapantsios [a,b,*], S.N. Raphaelides [a]

[a] *Food Process Engineering Laboratory, Department of Food Technology, Technological Educational Institution of Thessaloniki, University Box 14561, Thessaloniki 541 01, Greece*

[b] *Division of Chemical Technology, Department of Chemistry, Aristotle University of Thessaloniki, Box 116, Thessaloniki 540 06, Greece*

Received 2 March 2001; accepted 19 September 2001

Abstract

This work is concerned with the thermal field inside the pool of a starch slurry that preheats and gelatinizes between the drums of a double drum dryer. Experiments are conducted at several steam pressures, drum rotation speeds and levels of the pool between the drums. Temperature time records are employed as a means of studying the effect of all variables to the thermal distribution in the pool. Measurements indicate that subcooled boiling may be the dominant mechanism for heat transport in the pool.

Keywords: Drum drying; Pregelatinized starch; Temperature measurement; Time series analysis; Subcooled boiling

1. Introduction

Drum dryers are used to dry a wide variety of heavy pastes and thick liquids in both the food and chemical industries. A partial list of typical materials dried are precooked breakfast cereals, dry soup mixtures, yeast, various fruit purees, polyacrylamides, sodium benzoate, various propionates, various acetates, and many other chemical products (Moore, 1995). Among this variety of products the production of pregelatinized starch is a common industrial practice (Bonazzi et al., 1996). Double drum dryers are especially applicable in this process because of their ability to handle a wider range of products, better economics, more efficient operations, higher production rates and fewer operating labor requirements (Moore, 1995).

A double drum dryer consists of two cylinders (drums) of equal diameters rotating very close together in opposite directions, Fig. 1. The heating medium is usually saturated steam, introduced to the inside of the drum and condensed on the drum wall. The starch suspension is fed into the wedge shaped space between the drums (henceforth the pool) by means of a distribution pipe. Under the influence of the heat transferred from the hot drum surfaces to the starch suspension in the pool, the starch gelatinizes and swells to form a viscoelastic fluid (Fritze, 1973). The rotation of the cylinders causes the material in the pool to pass through the narrow space between them (henceforth the gap) and divides it into two films; one on each drum. This film is no longer in motion relative to the drums because of the rapid drying and solidification. After traveling part of a revolution, the dried film is removed in the form of thin sheets by scraper (''doctor'') blades spanning the whole width of the drums.

There are five variables involved in the operation of a double drum dryer on a given material:

1. steam pressure;
2. speed of rotation;
3. gap between the drums;
4. pool level between the drums; and
5. condition of the feed material, that is, the concentration, physical characteristics, and temperature at which the material reaches the drum surface.

A survey of the recent literature shows that studies dealing with double drum dryers are rather scarce and are mainly of technological interest, e.g. Kitson and MacGregor (1982), Rosenthal and Sgarbieri (1992). On

* Corresponding author. Tel.: +30-31-791-373; fax: +30-31-791-360.
E-mail address: karapant@cperi.certh.gr (T.D. Karapantsios).

0260-8774/02/$ - see front matter
PII: S0260-8774(01)00184-4

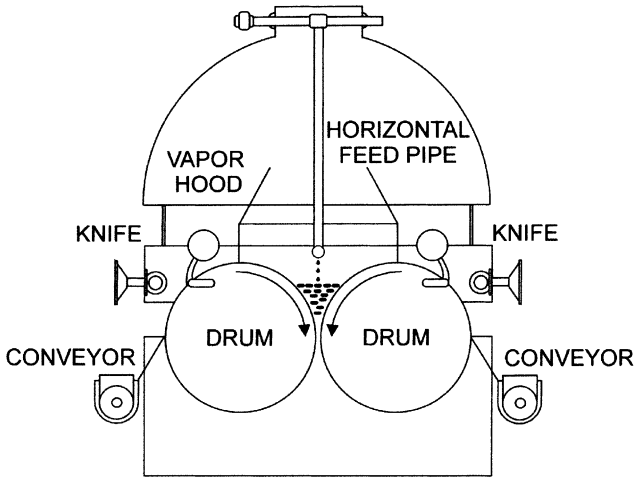

Fig. 1. Schematic representation of a top loading double drum dryer (GOUDA).

the other hand, several studies in the past have dealt with the performance of single drum dryers, e.g. Bonazzi et al. (1996), Daud (1988), Daud and Armstrong (1987), Rodriguez, Vasseur, and Courtois (1996), Trystram and Vasseur (1992). Among them, the work of Daud (1988) has some relevance to the present study since it investigates the flow behavior of the liquid in the pool before the material is extruded into a thin film and dries. However, direct comparison with the work of Daud is not possible because of the different geometries of the drum dryers and also because of the very small height (2.54 cm) of the liquid pool in his single drum dryer.

In order to obtain reliable information for commercial design purposes, tests must be performed on sufficiently large equipment to yield results that are characteristic of commercial size dryers. Because there are so many operating variables, as well as such a wide variation in product characteristics, it is impossible to make any definite prediction of drum dryer performance without either prior experience on the specific product or by conducting test work (Gardner, 1971; Moore, 1995).

In this paper we analyze temperature time-records acquired inside the liquid pool of a small-scale industrial double drum dryer. This is done in order to gain insight on the complex transport phenomena occurring in the pool, before the material is applied over the drums. The possible relation of the input variables (steam pressure, rotation speed, pool level) to the flow and thermal field in the pool is examined. The exceeding interrelationships among these input variables and output variables like drum temperature, product moisture and flow rate have been extensively reported in a previous publication (Vallous, Gavrielidou, Karapantsios, & Kostoglou, 2001). Here only the general trends are repeated to assist interpretations. Industry frequently encounters problems with the output product quality because of perturbations in moisture content (Rodriguez et al., 1996). The extent to which the phenomena occurring in the pool can affect subsequent drying and product quality is a matter of concern. To the best of our knowledge this is the first time that such a question is addressed regarding the performance of a double drum dryer.

2. Factors affecting liquid distribution inside the pool

The readily recognizable driving forces for fluid homogenization inside the pool are the rotation of the drums and gravity. It is well known that gelatinization leads to swollen particles which, under a shearing action, may exhibit a peculiar viscoelastic behavior (Doublier, 1981; Wong & Lelievre, 1981). This is even more so if one considers that the boundaries of swollen starch granules are not rigid but can deform considerably (Evans & Haisman, 1979). At every instant the pool accommodates a mixture of a small amount of (fresh) ungelatinized starch–water suspension and abundant quantities of gelatinized slurry. Since the fluid currents that can convect heat within the pool are slow, this mixture does not have a uniform temperature throughout and, consequently, its physical and rheological properties vary with both space and time. The complexity of the physical system is not easily amenable to a rigorous theoretical analysis and it is not our intention to attempt it at present. Even the much simpler case, where just a non-isothermal Newtonian fluid is present in the pool between two rotating drums, has not been treated so far. Here the main forces are recognized, which interact toward the establishment of a liquid distribution pattern. Their relative significance can be assessed by means of appropriate dimensionless numbers.

In order to characterize the dispersion of the just-fed-in starch suspension (low viscosity) into the already gelatinized starch in the pool (high viscosity), one may have to distinguish between even liquid distribution on a large scale (throughout the available volume) and uniform dispersion on a small scale (in the interstices between the swollen starch granules). Thus, two length scales can be readily identified, i.e. the pool effective radius given as $R_{\text{eff}} = V^{1/3}$, where V is the volume of the pool and the swollen granules radius r_{g}, representative of the large and small scales, respectively. To a first-order approximation the pool effective radius can be replaced by the drum radius, $R_{\text{eff}} \cong R$. It should be pointed out that an even suspension distribution on the large scale might be associated with more than one dispersion patterns on the small scale. Therefore, the fluid in the pool may not be as uniform as one would intuitively expect. This is in accord with the observations by Daud (1988), Fritze (1973) and Karapantsios, Sakonidou, and Raphaelides (2000).

Table 1
Typical values of force ratios for the starch slurry inside the pool between the two drums

Force ratio	Force proportionality	Dim/less number	$L = R = 0.25$ m	$L = r_g = 40 \times 10^{-6}$ m
Gravitational/capillarity	$\propto (L^3(\rho_\ell - \rho_g)g)/L\sigma$	Bond	10.4×10^3	0.27×10^{-3}
Viscous/capillarity	$\propto (L\mu V_{\text{eff}})/L\sigma$	Capillary	22	22
Inertial/viscous	$\propto (L^2\rho_\ell V_{\text{eff}}^2)/L\mu V_{\text{eff}}$	Reynolds	3.3	0.53×10^{-3}
Inertial/gravitational	$\propto (L^2\rho_\ell V_{\text{eff}}^2)/L^3(\rho_\ell - \rho_g)g$	Froude	7.0×10^{-3}	44
Inertial/capillarity	$\propto (L^2\rho_\ell V_{\text{eff}}^2)/L\sigma$	Weber	73	11.7×10^{-3}
Gravitational/viscous	$\propto (L^3(\rho_\ell - \rho_g)g)/L\mu V_{\text{eff}}$	Reynolds/Froude	0.47×10^3	0.012×10^{-3}
Order of significance			$\text{Gr}^{\text{O(100)}} > \text{In}^{\text{O(1)}} > \text{Vi}^{\text{O(10)}} > \text{Ca}$	$\text{Vi}^{\text{O(10)}} > \text{Ca}^{\text{O(100)}} > \text{In}^{\text{O(10)}} > \text{Gr}$

Table 1 includes a few well known dimensionless groups, such as the Bond (Bo), capillary (Ca), Reynolds (Re), Froude (Fr) and Weber (We) numbers, reflecting the relative significance of gravitational, capillarity, viscous and inertial forces. In addition, the ratio of Reynolds to Froude number is given. Due to paucity of information regarding the elastic forces associated with the pool material, the present analysis does not include such forces. Both numbers for the pool length scale and the swollen granules length scale are presented for comparison. An effective rotational speed, $V_{\text{eff}} = \omega R$, is employed only as a rough measure of the liquid velocity relative to the rotating drums.

To obtain order-of-magnitude estimates, typical values of the various dimensionless numbers are listed in Table 1 for a rotation speed of 5 rpm ($V_{\text{eff}} = 0.13$ m/s), which is within the range of our tests. The liquid density is taken equal to 1020 kg/m^3, which is an approximate average value calculated from in situ specific gravity tests. The viscosity of the gelatinized starch (10% w/w solids) is taken as ~10 Pas at $T = 95$ °C, a value inferred from the data published by Xu and Raphaelides (1998) for the same maize starch. The surface tension is that of water, ~60 mN/m at $T = 95$ °C (Straub, Rosner, & Grigull, 1980), since there is evidence that its value is practically not altered by starch polysaccharides (Raphaelides, 1986; Svenson, Gudmundsson, & Eliasson, 1996). An appropriate value for the swollen granules diameter is taken from Okechukwu and Rao (1996) and Ziegler, Thompson, and Casasnovas (1993) and is ~40 μm.

What is perhaps most interesting in Table 1 is that the rotation of the drums (inertia forces) does not govern the large-scale dispersion inside the pool since gravitational forces are markedly more important followed afar by inertia and viscous forces which appear to be able to compete effectively with each other. This, of course, is better interpreted not by assuming that gravity is so significant in this case but rather that the motion of the drums plays only an inferior role in promoting liquid distribution in the pool. This is contrary to the findings for partially filled with water rotating tubes (Karweit & Corrsin, 1975) and rotating packed beds (Karapantsios, Tsochatzidis, & Karabelas, 1993) where centrifugal forces clearly dominate over viscosity effects. The situation is somehow different on the small scale. The influence of viscous and capillary forces is evidently more significant compared to inertial and gravitational forces.

The above order-of-magnitude estimates lead to the following picture: Centrifugal forces are not so capable for bulk liquid movement. This is more so if one considers that far away from the drums the employed rotational speed, V_{eff}, is largely diminished due to the high viscosity of the mixture. Gravity evidently tends to promote liquid distribution on the large scale, R, but it appears that still another mechanism, other from those mentioned above, must be taken into account in order to explain liquid agitation in the pool. On the other hand, viscous forces and capillarity enhance liquid dispersion on the length scale of the swollen granules, r_g. It is necessary at this point to examine experimentally the liquid flow field in the pool and make comparisons with the present analysis.

3. Materials and methods

Commercial maize starch was purchased from Group Amylum S.A., Greece, with an initial moisture content of 13.5%. The total amylose content was 26.0 ± 0.3%, determined by the method of Morrison and Laignelet (1983). The volumetric granule size distribution, as determined in starch suspensions at 20 °C using a Malvern MasterSizer (Malvern Instruments Ltd.) laser diffraction particle size analyzer, is essentially unimodal over the range 6 to 30 m with only a very small fraction of particles below 3 μm. The granules mean diameter is 14.95 μm with a standard deviation of 5.8 μm.

Native maize starch is modified by a double drum dryer (GOUDA), Fig. 1. The drums have 0.5 m diameter and 0.5 m length and are synchronously driven at 4, 5 or 6 rpm. The drums are internally heated by steam at 6, 7 or 8 bars. The level of the free surface of the liquid pool between the two cylinders is meticulously regulated at 14, 18, or 22 cm above the gap (0.9 mm gap setting at ambient conditions). Starch/water suspensions with solids concentration of 10% w/w are employed as the dryer feed. The effects of steam pressure, drum speed and pool level are evaluated one variable at a time with the other variables held constant. Although this method

does not give a complete response surface (which would require keeping constant the output variables, i.e. product moisture and flowing rate), it does give essential information of the nature of the individual response which is useful for further experimental design. Such an experimental approach has been also used in the past, e.g. Straub, Tung, Koegel, and Bruhn (1979).

A complete set of temperature measurements, to obtain liquid temperature time records, is conducted using K-type thermocouples protruding into the pool liquid at selected locations, A, B, C_1, C_2, Fig. 2. The thermocouples are made of 0.5 mm diameter wire. The size of the thermocouples tip, ($\sim$1 mm), permits reliable local measurements only in the length scale of the overall liquid pool and not in the microscale between swollen particles. The way to position the thermocouples and their relative location is a matter of concern. It is apparent that a thermocouple rigid-stem projected perpendicular into a moving liquid layer can create a wake that may alter the local flow field, and it is uncertain at what downstream distance this effect vanishes. That is why, it was decided to insert the thermocouples stems vertically – on the same plane with the liquid 2D bulk motion – and keep a reasonable distance from each other. Measuring station A is located along the vertical axis of symmetry of the pool and only 3 cm above the gap. Its coordinates in centimeters in the 3D Cartesian system of Fig. 2 are ($x = 0,\ y = 3,\ z = 25$). Station B is 4 cm above and 3 cm off the vertical stem of thermocouple A ($x = 0,\ y = 7,\ z = 28$). C_1 and C_2 are placed in diametrically opposite positions very near the drums, C_1: ($x = -2,\ y = 12,\ z = 25$) and C_2: ($x = 2,\ y = 12,\ z = 25$). Their radial distance from the surface of the drums is calculated as 0.94 cm.

All thermocouples are calibrated to ± 0.1 °C at a certainty of 95%. The output from the thermocouples is sampled every 1 s. This sampling interval is adequate for the time constant of the thermocouples employed. Temperature readings are acquired for periods up to 90 min. Repeatability checks are made for each set of conditions, giving satisfactory results. Data are recorded using an ADAM 4018 16 bit A/D board (Advantech) interfaced to a PC. This leads to an error in the temperature readings of ± 0.2 °C within a 95% confidence interval. Pearson product–moment correlation coefficients are calculated to determine the extent of linear associations among the principal variables of the study. We must stress here that temperature measurements beside their own virtue is perhaps one of the most reliable way to get information about the flow field in the pool since it is not possible to make either direct optical measurements or use hot wire probes. This is so because the gelatinized slurry is opaque, very viscous and sticky.

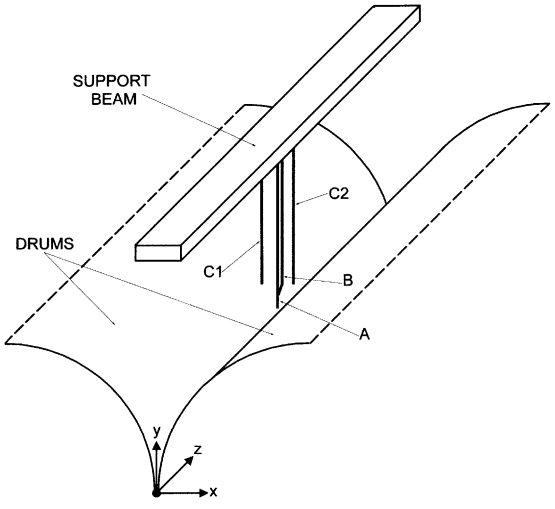

Fig. 2. Geometry of liquid pool and measuring thermocouples with coordinate system.

4. Method of data interpretation

Let $T(t)$ be a time series of temperature data measured at a fixed station inside the liquid pool. Temperature readings obtained simultaneously from the four measuring stations for a specific set of the dryer's operating conditions are presented in Fig. 3. The gross features of the traces obtained at stations B, C_1 and C_2 are quite alike and lie in the same range of values. On the contrary, the time record from station A is different not only regarding the values of the data but also the appearance of the signal. For instance, a common low frequency component is readily recognized in stations B, C_1 and C_2 but not in A.

One can easily discern two distinct random components in the measured temperature signals: high frequency oscillations superimposed over low frequency undulations. Such data can only be described as random or stochastic since there is no deterministic way to predict their exact value at any instant of time. Stochastic processes may be categorized as being either stationary or non-stationary; the former can be further categorized as either ergodic or non-ergodic (Bendat & Piersol, 1986). Only in the case that a time history record of a measured quantity is stationary and ergodic, then the standard time series analysis procedures can be employed to deduce information about these data. The concept of stationarity and ergodicity relates to the ensemble averaged properties of a random process and in practice means that the properties computed over short time intervals do not vary significantly from one interval to the next and are equal to the corresponding ensemble averaged values (Bendat & Piersol, 1986).

Employing time series analysis the following statistical properties of the data are obtained: Mean, T_m, and standard deviation, σ_T, of the record, representing the central tendency and dispersion of the data. The coefficient of variation, σ_T/T_m, as a measure of the variability

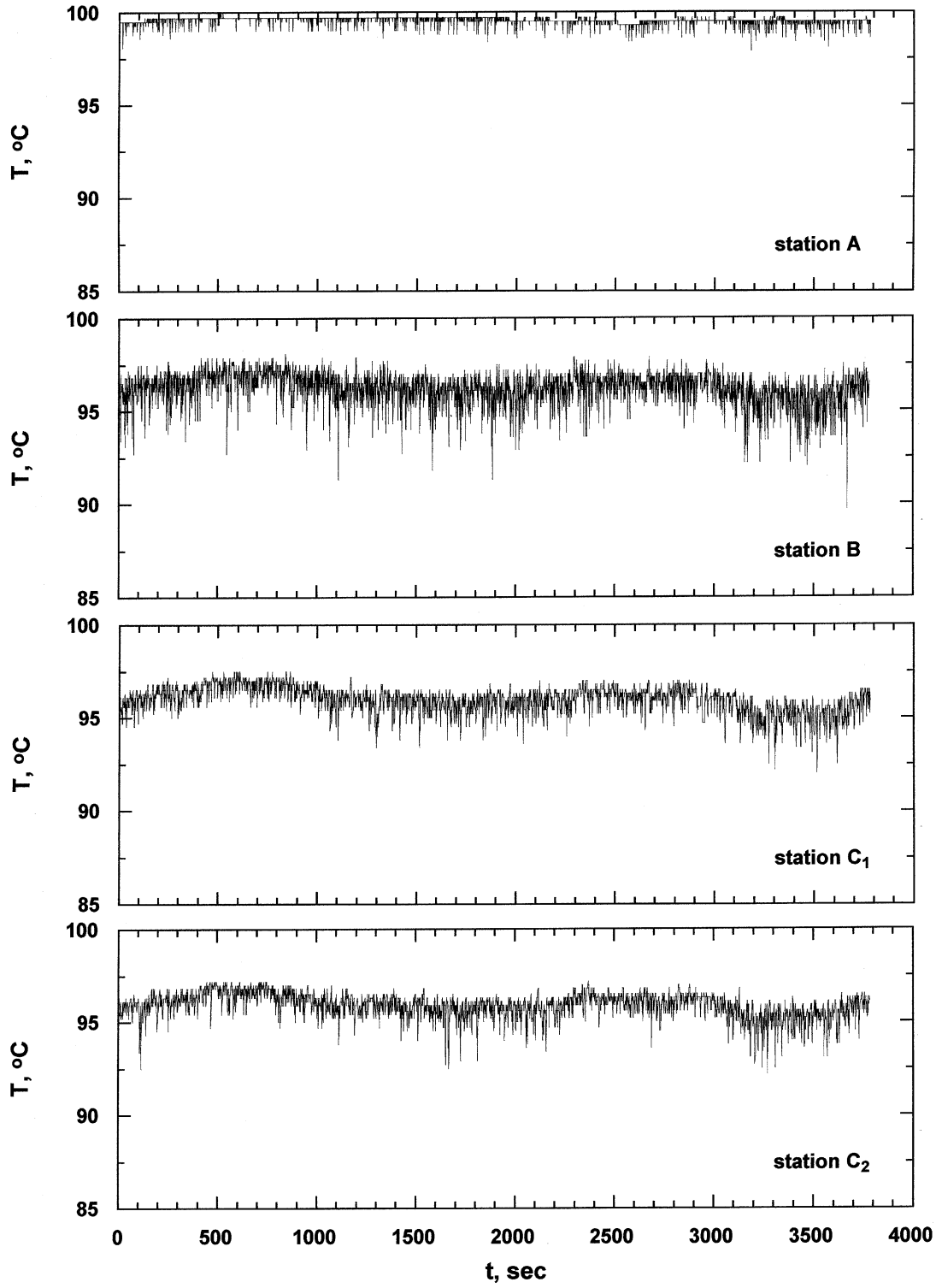

Fig. 3. Example of temperature time history records obtained at the four measuring stations A, B, C_1 and C_2 for the following operating conditions of the dryer: 6 bar steam pressure, 22 cm pool level and 4 rpm drum speed.

of the data about their mean value. The coefficient of skewness, α_3, and the coefficient of kurtosis, α_4, representing the shape of the probability density distribution (PDD) in terms of its deviation from the normal distribution. The coefficient of skewness is a measure of the asymmetry of the PDD whereas the coefficient of kurtosis expresses the degree of "peakedness" or "flatness" of the PDD. For a Gaussian distribution $\alpha_3 = \alpha_4 = 0$. These coefficients, beyond the basic evaluation of normality, allow for identification of non-linear effects and

analysis of extreme outlier values. Finally, the autocovariance function, $C_T(r)$, and the spectral density function, $G_T(f)$, which permit detection of periodicities, measurement of time delays and identification of propagation paths. These quantities are defined below (e.g., Derman, Gleser, & Olkin, 1973):

$$\alpha_3 = \frac{m_3}{m_2^{3/2}}, \tag{1}$$

$$\alpha_4 = \frac{m_4}{m_2^2}, \tag{2}$$

$$C_T(r) = \lim_{\Delta t \to \infty} \frac{1}{\Delta T} \int_0^{\Delta T} (T(t) - T_m)(T(t+r) - T_m)\mathrm{d}t, \tag{3}$$

$$G_T(f) = \int_{-\infty}^{\infty} C_T(r) \mathrm{e}^{-\mathrm{j}2\pi fr}\,\mathrm{d}r, \tag{4}$$

where m_i is the ith central moment of the data, ΔT is the sampling period, r is the time interval of calculations and f is the frequency. An assumption for stationarity can often be supported by a simple non-parametric test of sample mean square values computed from the available data. In particular, time invariance of mean and mean square values is often sufficient to warrant stationarity. The mean square value, ψ_T^2, equals the variance, σ_T^2, plus the square of the mean. More strictly speaking, the individual sample record is said to be stationary in the case where the standard deviation and autocovariance function do not vary significantly as the starting time varies.

The data in Fig. 3 as well as all other data of the present work – meet the requirements for stationarity and ergodicity in a wide sense (*weakly stationary*). In principle, weakly stationary data such as those in Fig. 3 might be also viewed as almost-periodic deterministic data, stochastic data including spurious trends or non-stationary data (Bendat & Piersol, 1986). Summing together several sine waves of arbitrary frequencies (almost-periodic deterministic data) is potentially able to produce the general appearance of the traces in Fig. 3. Thus, the seemingly random time records of Fig. 3 might simply represent the mixing-up effect of several unrelated periodic phenomena. Calculating the autocovariance and spectral density functions, Eqs. (3) and (4), of the present data gave responses similar to a wide band random noise, with no indication whatsoever of any dominant periodicities.

Situations sometime arise where the sampled stochastic data include spurious trends or low frequency components with a wavelength comparable or longer than the record length. Such low frequency components are apparent in Fig. 3. Common sources of spurious trends are data collection instrumentation drift and signal integration operations. Problems of this kind are not expected to occur in this work. Besides, the simultaneous appearance of these trends in the independently sampled records at the four measuring stations supports strongly the notion that the measured trends are not an experimental artifact.

The low frequency trends in Fig. 3 might also reflect a non-stationary random process consisting of stationary functions superimposed over a deterministic time trend. This could be effectively described by a composite function, $T(t) = \alpha(t)u(t)$. Here, $u(t)$ is a sample function from a stationary random process and $\alpha(t)$ is a deterministic multiplication factor. In such cases, statistical values are estimated by operations equivalent to low pass filtering. As such, the method of the segmented mean value estimates is often preferred for simplicity, which calls for short time-averaging operations. Copious calculations by this method with the present data did not yield persistent time trends among the various experimental conditions so an appropriate multiplication factor, $\alpha(t)$ was not identified.

To this end, the stochastic process of temperature fluctuation can be considered as effectively (weakly) stationary and ergodic. The sample size (time length) providing representative statistical averages is determined next. The propagating mean temperature value, $T_m(0 \to t)$, is used as a criterion to judge the adequacy of sample size. It is seen that the time to reach a quasi-steady-state thermal condition inside the pool is always above 10 min. However, often 20–30 min and in some occasions even more than 60 min are required to arrive at steady state. This slow equalization is chiefly a result of the signal's low frequency components. Similar observations were made by Vasseur and Loncin (1983) who incorporated about 12 rotations in their unstationary heat transfer model in order to reach a reasonable pseudo-stationary state for the surface temperature of the drums. Experimental evidence from this and previous work (e.g. Wang, Qiu, & Wang, 1990) shows that sporadic irregularities in steam supply or steam traps operation may be reflected as low frequency components at the temperature signals in the pool. It must be mentioned here that the possible convective currents created by the motion of the drums inside the pool will naturally have a much shorter time scale (15–12 s for 4–6 rpm). So, the rotation of the drums could affect only the higher frequency temperature components.

5. Results and discussion

5.1. Average residence time of material inside the gelatinization pool

Simple analytic geometry leads to the following expressions for the pool volume (V) and the horizontal

separation distance between the drums at the free surface of the pool (S):

$$V = L\left\{2\left(R+\frac{d_o}{2}\right)H - \left(R^2-H^2\right)^{1/2}H - \arcsin\left(\frac{H}{R}\right)R^2\right\}, \quad (5)$$

$$S = 2\left\{\left(R+\frac{d_o}{2}\right) - \left(R^2-H^2\right)^{1/2}\right\}, \quad (6)$$

where L is the drum's length, R is the drum's radius, H is the level of the free surface of the pool (distance from the gap), d_o is the width of the gap. Fig. 4 presents the variation of V and S with respect to the vertical distance from the gap ($d_o = 0.3$ mm). A strongly non-linear behavior is observed for both quantities which indicates serious deviations in heat and mass transport phenomena occurring at different pool levels.

Knowledge of the throughput rate of the dryer and the pool volume can give the residence time of the pregelatinized starch in the pool. For the specific pool levels encountered in this study, 14, 18 and 22 cm, the pool volumes are estimated from Eq. (5) as 1950, 4300 and 8350 ml, respectively. The residence time in the pool reflects the period the material spends for gelatinization. Spatial inhomogeneities in the bulk density, moisture and temperature of the material in the pool permit only estimations of average residence times. For the employed experimental conditions, the calculated residence times vary approximately between 3 and 15 min, Fig. 5(a) and (b). The shorter times correspond to lower pool levels, higher rotation speeds and lower steam pressures. It appears, though, that the pool level is the dominant parameter among the three. The role of the residence time in the pool as regards the degree of gelatinization and dry product rheological and physical characteristics has been dealt with in another study (Anastasiades, Thanou, Loulis, Stapatoris, & Karapantsios, 2001).

It is important to mention here that average residence times are representative of the processing time in the pool only if there is adequate mixing of the material in the pool. In cases of a residence time distribution or a bad mixing in the pool the associated material flow rate will not be adequately characterized by the average residence time. Daud (1988) used a salt tracer technique to investigate the non-ideal flow behavior in the small pool of a single drum dryer. His effort was hampered by several experimental constraints (non-constant flow rate of tracer, volumetric expansion due to swelling of starch granules, indirect method to detect the tracer in solid product) which affected the accuracy of the measured residence time distribution curves. These curves lead him to a non-ideal flow model for the dryer consisting of a parallel combination of a bypass and an ideal stirred tank with a dead volume attached to the latter. Comparisons with the present double drum dryer cannot be made due to the very different scales of the pools and the different properties of the feed material. The overall uncertainty in measurements discouraged us from undertaking a similar effort.

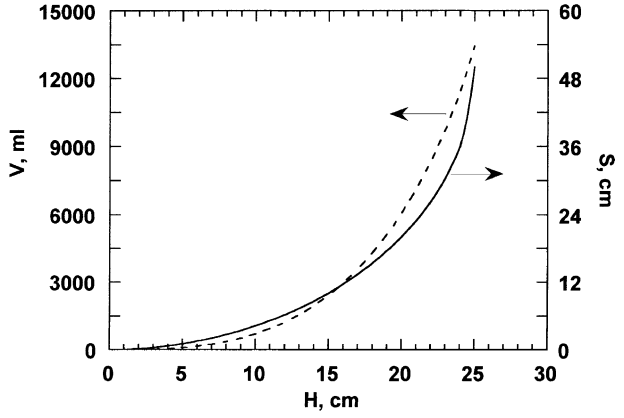

Fig. 4. Variation of pool volume (V) and horizontal separation distance at the free surface (S) versus pool level (H).

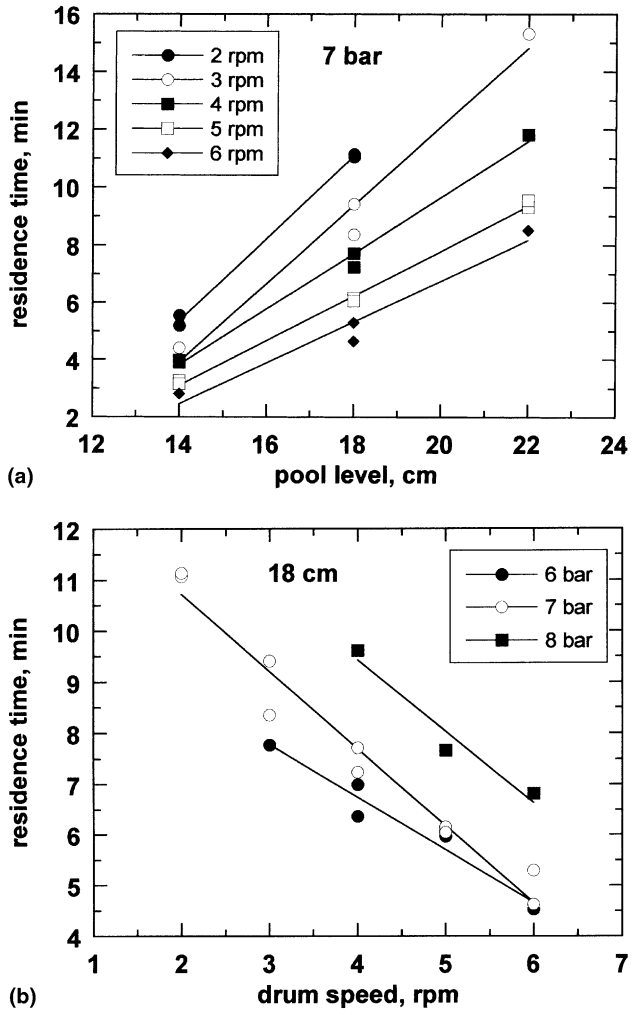

Fig. 5. Residence times of material inside the gelatinization pool versus (a) pool level and (b) rotation speed.

5.2. Preliminary observations

The free surface of the liquid pool is never calm. The less liquid in the pool the more disturbed is its free surface. Surface agitation is chiefly attributed to boiling activity. At first sight the boiling activity at the surface seems contradictory to the low temperatures of the bulk presented in Fig. 3 (more about this later). The arrival (and burst) of vapor bubbles at the free surface is much more evident at lower pool levels. This is rather expected since then the material is confined at a narrower wedge between the hot rotating walls and as a result boiling activity can have a higher influence on the liquid masses. On the other hand, the rotation of the drums has a smaller effect on the agitation of the pool due to the high viscosity of the liquid mixture. This is clearly manifested in the direction of flow at the free surface of the pool. Should the rotation of the drums be dominant, flow on the free surface would be directed from the centerline of the pool towards the moving drums. However, exactly the opposite is observed for all experimental conditions. That is, the viscous gelatinized layers of the surface move from the sides of the pool towards its center. There, they mix with the low viscosity cold feed and together immerse vertically into the pool. The observed direction of surface flow is compatible with surface tension thermal gradients but it is really doubtful whether thermo-capillary forces can prevail over the significant viscous stresses at the surface.

At the contact line between the free surface and the drums the gelatinized material performs an intense short-living motion: for a split second it bounces away from the drum walls and then pulls back to adhere again to the walls. For as long as the liquid is temporarily detached from the walls, vapor accumulating between the drums and the liquid escapes to the environment. This repeated activity looks like the up-and-down motion of a lid covering a kettle with boiling water inside. During this motion the gelatinized layers at the edge region of the free surface behave like an elastic membrane that compresses and expands accordingly.

A possible explanation for the above observations may be as follows. The vapor production rate from the material in contact with the drum walls is higher than the rate of vapor (bubbles) removal and as a result there is a predominance of vapor over the wall. This is so because the high viscosity of the liquid in the pool retards bubble departure and hence a continuous vapor film has time to develop. This condition is not unusual and is generally known as *vapor blanketing* (Kern, 1950). Growing vapor bubbles coalesce and soon turn into a continuous gas film that increases its temperature and pressure. It is this overpressure that temporarily pushes the gelatinized layers away from the drum wall and offers a path for the vapor to escape. The existence of vapor between the material and the drum surface has been also reported in the past either as an additional thermal resistance to heat up the pool material, (Wang et al., 1990), or as a barrier preventing uniform adherence of the product to the drum surface (Moore, 1995).

5.3. Effect of steam pressure on pool temperatures

According to Vallous et al. (2001), when the steam pressure inside the drums increases the temperature of the drum walls globally increases, too. Consequently, the drums expand and as a result the width of the gap between the drums gets narrower. These two actions were found to reduce the mass flow rate, film thickness and moisture of the end product. It must be noted here that the temperature of the drum surface is not constant around the circumference but varies substantially with angular location e.g., Abchir, Vasseur, and Trystram (1988), Vasseur, Abchir, and Trystram (1991). This was attributed to the non-uniform heat fluxes throughout the rotation, which from very high near the gap are largely diminished at the doctor blade position. Accordingly, the highest drum temperatures are achieved at sections where the drums are bare – no contact with material – whereas the lowest at sections near the gap.

Fig. 6(a) displays the variation of T_m with steam pressure inside the drums. Error bars represent the standard deviation of the recorded signal. The values for station A are quite stable around 99 °C and almost identical for all conditions. This value is quite close to the boiling temperature of the mixture which is expected to be a few degrees above 100 °C due to the presence of solids. The situation is rather dictated by the narrow geometry of the spot at station A where the drum walls are separated horizontally by only 3.9 mm (Eq. (6)) with only little material in-between. Most of the mean temperatures calculated for the other three stations are quite close together indicating a rather good thermal homogeneity in the central section of the pool where these stations are located. Moreover, these mean values show a positive tendency with steam pressure for all speeds of rotation. This is rather expected due to the higher energy that is supplied through the drum walls at higher pressures as is also manifested by the higher drum temperatures (Vallous et al., 2001).

The higher T_m values correspond to the lower σ_T values. This is better shown in Fig. 6(b). Pearson coefficients close to −0.9 for all stations, except for A where the coefficient drops to −0.5, ascertain the strong negative correlation between T_m and σ_T. Combining the above implies that at higher steam pressures the thermal field at the specific locations of the measuring stations is more uniform. This can be probably attributed to the lower viscosity of the liquid mixture at elevated temperatures, which facilitates bubble rise and convective heat transport. Furthermore, for the vast majority of the present time records the coefficient of variation is below

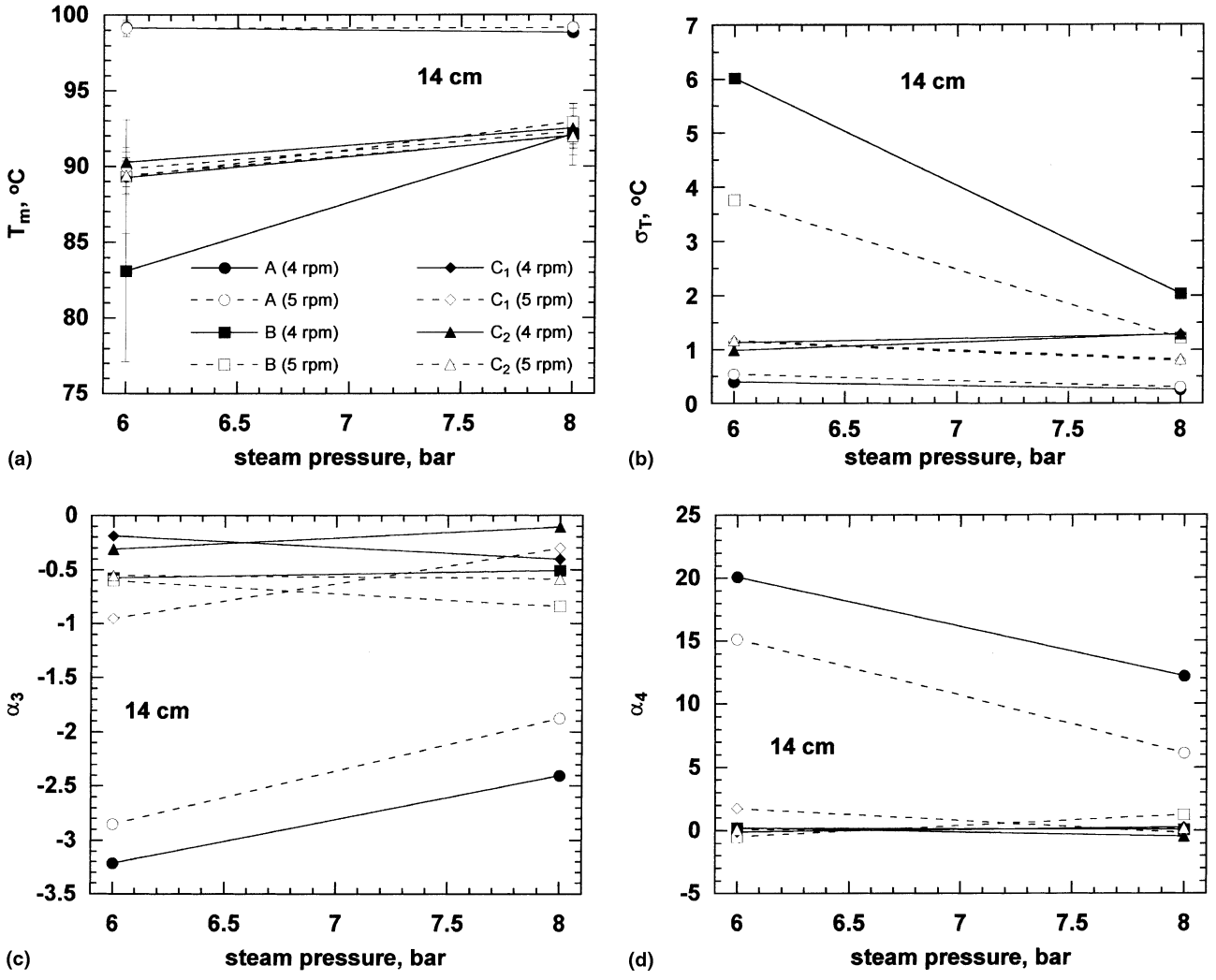

Fig. 6. Effect of steam pressure on the (a) mean temperature, T_m, (b) standard deviation, σ_T, (c) skewness, α_3, and (d) kurtosis, α_4, of the temperature records measured at the four measuring stations inside the pool. Data are for pool level 14 cm. The legend in plot (a) holds also for the other plots.

0.02 (max: 0.07) indicating that the obtained mean values are adequate representatives of the local temperature fields. Noticeably, the largest coefficient of variation values occur for measuring station B. This particular spot lies on the vertical axis passing through the cold feed entry and the gap and not far away from the free surface of the pool, especially for a pool level of 14 cm. Therefore, a low mean temperature combined with a high standard deviation possibly demonstrates that at this location appreciable mixing still takes place between hot and cold liquid masses (see also below).

Fig. 6(c) and (d) present the coefficients of skewness and kurtosis versus steam pressure. The distributions of the $T(t)$ time series from the four measuring stations are all skewed (asymmetric) to the left, $\alpha_3 \approx -0.1$ to -3.3, throughout the steam pressure range studied. Fig. 6(d) shows kurtosis values varying between $\alpha_4 \approx -1$ to 20. In most cases, a positive kurtosis is calculated, characteristic of a leptokyrtic PDD (many data around T_m). All the calculated PDDs do not satisfy the normality tests of Kolmogorov–Smirnov and $z_s = |\alpha_3|\sqrt{n/6} > 1.96$, $z_k = |\alpha_4|\sqrt{n/24} > 1.96$ where n is the size of the time record (Petridis, 1997). In very few cases, one of the criteria is marginally satisfied but the other is again negative for normality. Furthermore, the two coefficients have a considerable negative interrelation with Pearson coefficients above −0.8 for all measuring stations.

Data recorded at station A (Fig. 6(c)) are markedly asymmetric but improve as steam pressure rises whereas data from the other stations are comparable to each other and do not virtually vary with steam pressure. Regarding the kurtosis (Fig. 6(d)), data from station A are again far away from normality showing a negative variation with steam pressure. Kurtosis values up to 43 are calculated for other operating conditions (not shown) from data measured at A. Kurtosis values from the other three stations are closer to zero for all steam pressures.

The α_3 and α_4 values in combination with the T_m, σ_T and σ_T/T_m values reveal some important information about the thermal field at the measuring stations. The negative skewness indicates a possible rough pattern for the flow field: liquid lumps that instantaneously pass-by the thermocouples are under *transient heating-up* conditions as they travel from colder upstream regions towards hotter downstream ones (if the opposite happened a positive skewness would be observed). The PDDs obtained at station A have a long tail to the left, are sizably leptokyrtic and are characterized by a very low variability around the mean value. This implies that the thermal field at station A is quite stable most of the time but once in a while lower temperature spikes appear. Thus, the material in this region is in essence isothermal, presumably near the saturation temperature. The picture is different for the other measuring stations where the PDDs are much closer to the normal distribution. Specifically, their signals are negative skewed and for most cases moderately leptokyrtic but their dispersion about their mean value is always higher than in A. Apparently, the thermal field in these locations is characterized by alternating hotter and colder liquid masses of comparable temperature-spread around the T_m of the spots. The dynamic character of the field is more evident at station B where the undulations above and below T_m are intense. These arguments are in qualitative agreement with the general appearance of the traces in Fig. 3.

5.4. Effect of drum speed on pool temperatures

When the drum speed increases, the response of the double drum dryer is different for the different steam pressures employed (Vallous et al., 2001). At 6 and 7 bars, as the drum speed increases the width of the gap, product's moisture and mass flow rate go up whereas the drum temperature and film thickness go down. On the contrary, at 8 bars all variables are virtually invariant for the employed operating conditions.

Fig. 7(a) displays the impact of drum speed on the measured pool temperatures. It is apparent that for the employed speeds no significant variation is observed. The only exception is the record obtained at station B for 4 rpm where, however, a large standard deviation is calculated. It is quite probable that at such a low speed and level of pool (14 cm) the slow mixing of hot and cold masses in that region can cause these temperature variations. In all other measured records the low standard deviation indicate a more homogeneous local temperature field. In particular, the higher the mean temperature the lower the standard deviation, Fig. 7(b). It is apparent in Fig. 7(a) that the effect of pool level is more profound than that of steam pressure for the same speed of rotation.

Fig. 7(c) and (d) present the respective coefficients of skewness and kurtosis. Negative skewness and (mostly) positive kurtosis values are calculated with no obvious dependence on speed of rotation. Once more the signals obtained at station A depart more from symmetry. The other signals possess comparable PDDs features indicating again a rather homogeneous temperature field. On the whole, Fig. 7 demonstrates that for the employed speeds of rotation no significant variations occur in the thermal field of the pool. Fig. 7 alone does not allow estimating whether drum motion has just a small effect on liquid agitation inside the pool or its influence is already large enough and simply does not vary from one speed to the other. Yet, if one combines the aforementioned visual observations regarding the motion of the free surface of the pool and Fig. 7 then the first alternative is further supported.

5.5. Effect of pool level on pool temperatures

The height of the pool is a parameter that completely defines the geometry of the liquid accumulating between the drums, i.e. Eqs. (5) and (6). This geometry despite axisymmetric is largely non-linear in the 2D plane. Therefore, the height alone is not capable of describing sizably all relevant length scales that can play a role in momentum and heat transport inside the pool. Table 2 presents the most characteristic length scales of the system. H, S and V are the same as earlier while A denotes the surface area of the drums that is in contact with the pool material. All scale ratio decrease with increasing H except S/A. This is an indication that there may exist a reasonable qualitative resemblance regarding the transport phenomena at the three examined pool levels. Quantitatively speaking, large discrepancies are expected and for this a detailed examination is required which however is beyond the scope of this study.

The height of the pool prescribes also the residence time of the material between the drums and consequently its degree of preheating and gelatinization. Vallous et al. (2001) found that for the range 4–6 rpm as the pool level rises the surface temperature of the drums slightly drops (the gap widens) and the mass flow rate and film thickness of the end product increase. Regarding the product's moisture there is almost no effect except for speeds of 6 rpm (and higher) where moisture is found to increase with pool level.

Fig. 8 presents the dependence of the measured pool temperatures on pool level. Apart from the temperatures at station A, which are again high and similar to each other, there is a clear tendency for larger T_m values as the pool level increases, Fig. 8(a). This is so for all steam pressures and speeds of rotation. Once more, σ_T is inversely proportional to T_m, Fig. 8(b), and decrease with pool level. For reasons outlined before, the standard

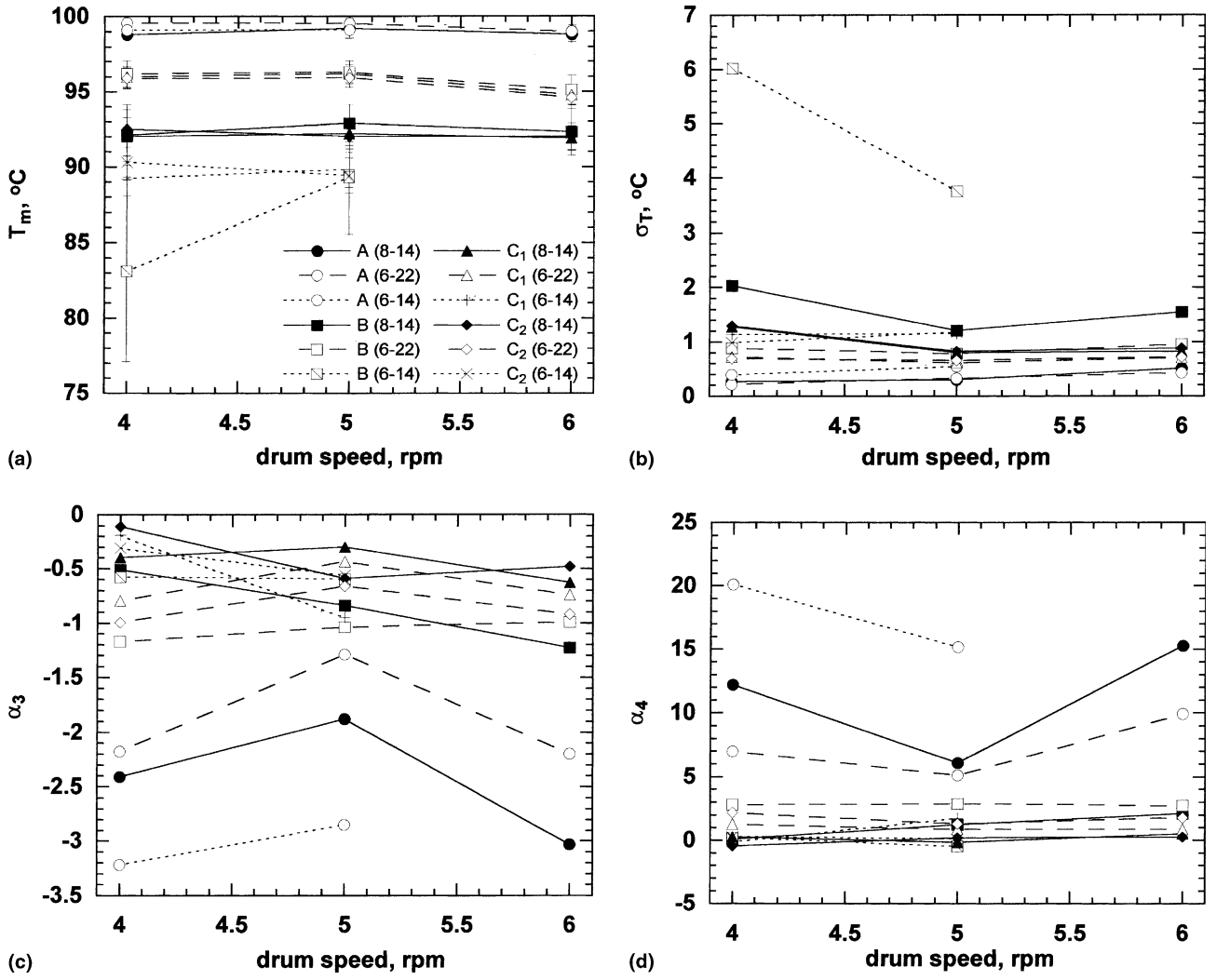

Fig. 7. Effect of drums speed on the (a) mean temperature, T_m, (b) standard deviation, σ_T, (c) skewness, α_3, and (d) kurtosis, α_4, of the temperature records measured at the four measuring stations inside the pool. The legend in plot (a) holds also for the other plots.

Table 2
Variation of characteristic length scales of the pool with respect to pool level

H (cm)	S (cm)	A (cm^2)	V (cm^3)	H/S	H/A (10 cm^{-1})	H/V (10^2 cm^{-2})	S/A (10 cm^{-1})	S/V (10^2 cm^{-2})	A/V (cm^{-1})
14	8.61	745	1950	1.63	0.19	0.72	0.12	0.44	0.38
18	15.33	1005	4300	1.17	0.18	0.42	0.15	0.36	0.23
22	26.28	1345	8350	0.84	0.16	0.26	0.20	0.31	0.16

deviations calculated from data at station B are significantly larger than the rest. The variation in the PDDs of the measured signals is presented in Fig. 8(c) and (d). Distributions at station A are largely non-canonical but improve as the pool level increases. Exactly the opposite holds for the other stations where values are initially closer to the normal distribution and depart gradually with pool level.

If one combines information from Table 2 and Fig. 8 an interesting situation arises. For smaller heights of the pool, a larger A/V conventionally means a higher and more effective energy transfer from the drums to the liquid. This is even more so if one notes that the higher drum temperatures are attained at low pool levels, e.g. Vallous et al. (2001). The smaller H and S distances support further the enhanced heat transport inside the pool. In addition, a higher H/S value means that a larger fraction of material lies nearby the drum walls and is therefore more influenced by the hot rotating drums than at other pool levels. Despite all this, the

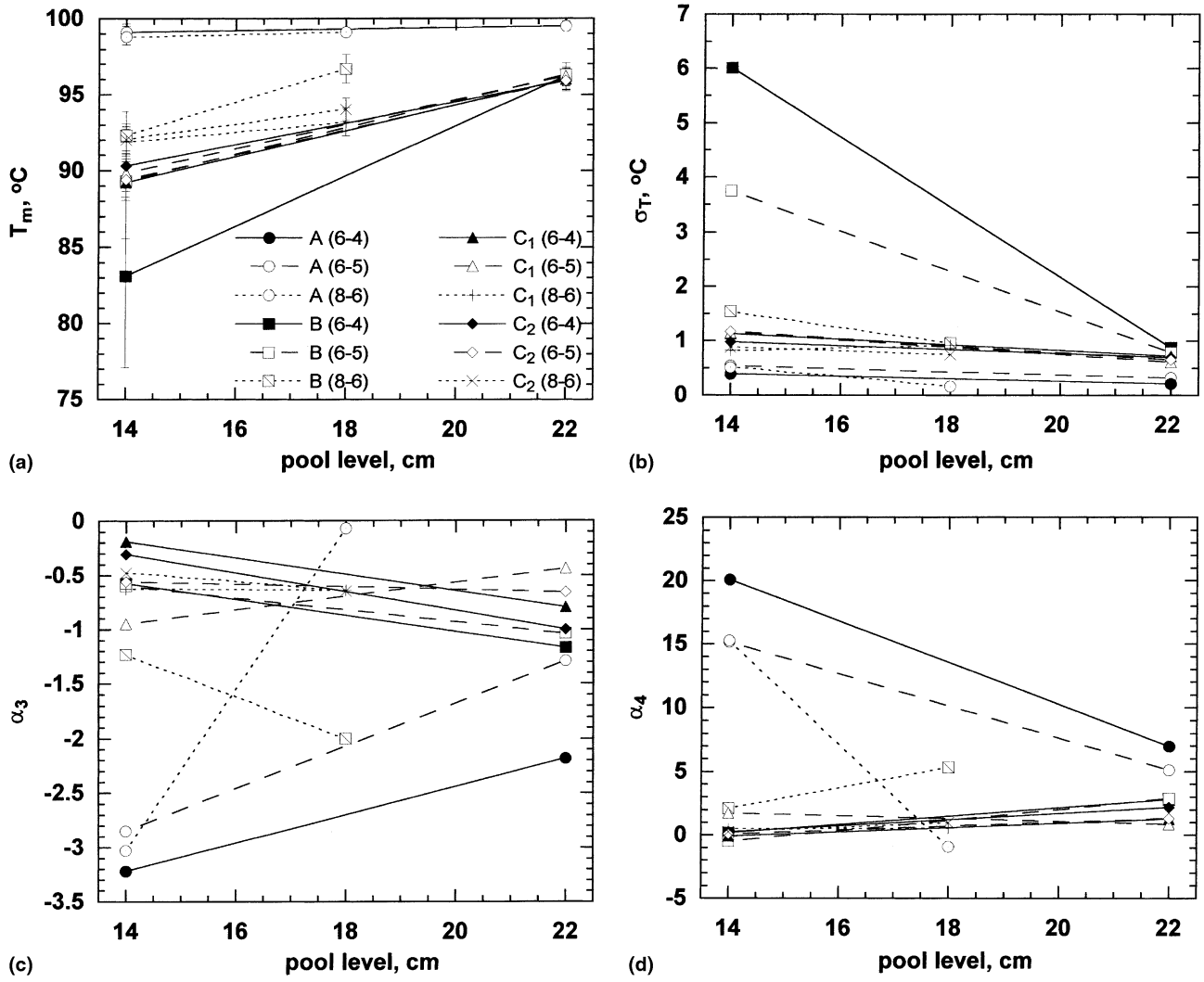

Fig. 8. Effect of pool level on the (a) mean temperature, T_m, (b) standard deviation, σ_T, (c) skewness, α_3, and (d) kurtosis, α_4, of the temperature records measured at the four measuring stations inside the pool. The legend in plot (a) holds also for the other plots.

mean temperatures obtained at all stations – apart from A – are smaller at lower pool levels!

For station B it can be argued that at low pool levels the smaller temperatures are due to the short distance between the measuring spot and the free surface of the pool from where the cold feed enters the pool. This argument is in accord with the visual observation that the just-fed-in low viscosity suspension does not dissipate around its entry point but dives vertically into the pool. But why the temperatures measured at C_1 and C_2 are also smaller? These stations are only about 1 cm off the drum walls and far away from the cold feed vertical streamline. The only possible explanation is that heat transfer from the walls is restricted by the presence of a barrier and as a result, the temperatures even so close to the drum walls are still influenced by the agitation of the liquid. A plausible barrier for heat transfer is the existence of a vapor layer over the drums surface due to local boiling. Such a gas layer was invoked earlier to explain the motion of the surface at the edges of the pool. When a blanketing gaseous film forms over the drums, energy transport is hindered because the liquid is not anymore in contact with the hot wall but with vapors at $T_{sat}(\sim 100\ ^\circ C)$. Also, it must not be disregarded that such a vapor layer will not permit the material to adhere to the solid walls and get dragged towards the gap. However, the latter is indirectly evidenced by experiments that relate strongly the mass flow rate of the end product with the speed of rotation (Trystram & Vasseur, 1992; Vallous et al., 2001). On the basis of all the above, the following possible physical picture emerges: from the free surface of the pool down to at least the location of measuring stations C_1 and C_2 practically no adherence is achieved between the drums and the pool material due to predominant local boiling which results in an intervening vapor layer. At some lower position, possibly quite close to the gap, the material in contact with the drums gets finally partly

solidified and eventually adheres to the drums. It is only after this position that the material is carried over by the drum motion through the gap.

If the above description is valid, this has a direct consequence on the drying phenomena occurring at a double drum dryer. Since a major moisture loss occurs before the material passes through the gap then the drum surface is covered by an already semi-dried paste when it exits the pool. Daud and Armstrong (1987) made similar observations and described the drying phenomena occurring after the gap by a mechanism similar to drying in capillary porous media. However, other investigators have overlooked this approach (Trystram & Vasseur, 1992; Vallous et al., 2001). The present results lend further support, although not conclusively, to the work of Daud and Armstrong (1987).

Not all the vapor escapes to the environment as a blanketing film from the sides of the pool but a sufficient number of *large* vapor bubbles ($d_b \approx 2$ cm) is also noticed to rise through the main body of the material. This is more evident at lower pool levels where many bubbles are observed to reach the free surface of the pool while the liquid appears vigorously agitated. Such an intense activity can by no means emerge by the drum rotation alone but must be also attributed to the convective currents produced by the rising bubbles. Assuming "creeping flow" (it is $Re < 0.1$) and using Stoke's law for an average bubble diameter of 2 cm, a terminal velocity of about 9 cm/s is calculated. This approximate value is comparable with the velocity imparted by the moving drum walls. Of course, due to the low depth of the pool there is no chance that the bubbles will reach their terminal velocity. Most of the bubbles are observed to ascent on the free surface not far from the central part of the pool. So, one might argue that they should be created on the section of the drum lying between the region of a blanketing film and the region of the gap where the solidified material adheres to the drums. These bubbles grow until they reach a critical size where buoyancy becomes large enough to overcome the viscoelasticity of the liquid above. In fact, due to the prominent viscoelastic behavior of the liquid mixture, bubble rise is hampered until the bubbles get appreciably large. It is quite probable that such large bubbles are the result not only of cumulative water evaporation but also of coalescence of neighboring bubbles.

The acquired temperature signals allow speculation about the possible heat transport mechanisms inside the pool. Apart from values obtained at station A, all other temperatures are well below the boiling temperature of the liquid mixture. Thus, *subcooled* boiling rather prevails in the pool. According to this, the rising vapor bubbles partially recondense (or even collapse) when they come in contact with colder masses, releasing large amounts of energy along their trace (Kern, 1950). In addition, some heat is convected to the bulk of the pool by flow currents induced by the rising bubbles and to a quite lesser extent by the rotation of the drums. It is inevitable that some heat is also transported by conduction (molecular transport) through the body of the mixture. Among the three mechanisms subcooled boiling is expected to dominate inside the pool but one should withhold final judgement until more evidence is acquired.

6. Conclusions

The present temperature data reveal useful information as regards heat transport inside the pool formed between the drums of a double drum dryer. Two characteristic length scales are recognized for fluid flow inside the pool. The size of the measuring thermocouples allow estimation of temperature distribution on the large scale (throughout the whole pool) but can not provide information relating to dispersion on the small (granule) length scale. Among the examined input variables (steam pressure, speed of rotation, pool level) the level of the pool appears to be more significant in terms of material agitation and thermal equalization. Measurements indicate that along the vertical axis of symmetry of the pool there are regions with intense mixing activity between alternating hot and cold masses. This is attributed to the observed descending flow trajectory of the cold feed suspension right after its entry in the pool. It appears that these cold masses can travel quite far below the free surface before finally thermalize and it is only near the gap that the material attains a temperature close to its boiling temperature. The present data indicate that apart from the region of the gap, subcooled boiling rather takes place in most of the liquid pool even very close to the drum walls and this is believed to be the major mechanism for heat transport inside the pool. Furthermore, the existence of a vapor layer blanketing a large part of the drum walls is assumed to explain the behavior of the recorded temperature data.

References

Abchir, R., Vasseur, J., & Trystram, G. (1988). Modelisation and simulation of drum drying. In *Proceedings of the Sixth International Drying Symposium, Versailles, France* (pp. 435–439).

Anastasiades, A., Thanou, S., Loulis, D., Stapatoris, A., & Karapantsios, T. D. (2001). Rheological and physical characterization of pregelatinized maize starches. *Journal of Food Engineering* (accepted).

Bendat, J. S., & Piersol, A. G. (1986). *Random data: Analysis and measurement procedures*. New York: Wiley.

Bonazzi, C., Dumoulin, E., Raoult-Wack, A., Berk, Z., Bimbenet, J. J., Courtois, F., Trystram, G., & Vasseur, J. (1996). Food drying and dewatering. *Drying Technology, 14*(9), 2135–2170.

Daud, W. R. b. W. (1988). Non-ideal flow model of a top loading drum dryer. In *Proceedings of the Sixth International Drying Symposium, Versailles, France* (pp. 77–86).

Daud, W. R. b. W., & Armstrong, W. D. (1987). Pilot plant study of the drum dryer. In A. S. Mujumdar (Ed.), *Drying '87* (pp. 101–108). New York: Hemisphere.

Derman, C., Gleser, L. J., & Olkin, I. (1973). *A guide to probability theory and apllications*. New York: Holt, Rinehart & Winston.

Doublier, J. L. (1981). Rheological studies on starch-flow behavior of wheat starch pastes. *Starch/Starke, 33*, 415–420.

Evans, I. D., & Haisman, D. R. (1979). Rheology of gelatinized starch suspensions. *Journal of Texture Studies, 10*, 347–370.

Fritze, H. (1973). Dry gelatinized produced on different types of drum dryers. *Industrial Engineering, Chemistry, Process Design and Development, 12*(2), 142–148.

Gardner, A. W. (1971). *Industrial drying* (pp. 220–242). London: Leonard Hill Books.

Karapantsios, T. D., Tsochatzidis, N. A., & Karabelas, A. J. (1993). Liquid distribution in horizontal axially rotated packed beds. *Chemical Engineering Science, 48*(8), 1427–1436.

Karapantsios, T. D., Sakonidou, E. P., & Raphaelides, S. N. (2000). Electrical conductance study of fluid motion and heat transport during starch gelatinization. *Journal of Food Science, 65*(1), 144–150.

Karweit, M. J., & Corrsin, S. (1975). Observation of cellular patterns in a partly filled, horizontal, rotating cylinder. *Physics of Fluids, 18*, 111–112.

Kern, D. Q. (1950). *Process heat transfer*. New York: McGraw-Hill.

Kitson, J. A., & MacGregor, D. R. (1982). Technical note: drying fruit purees on an improved pilot plant drum dryer. *Journal of Food Technology, 17*, 285–288.

Moore, J. G. (1995). Drum Dryers. In A. S. Mujumdar (Ed.), *Handbook of industrial drying* (Vol. 1, 2nd ed.). New York: Marcel Dekker.

Morrison, W. R., & Laignelet, B. (1983). An improved colorimetric procedure for determining apparent and total amylose in cereal and other starches. *Journal of Cereal Science, 1*, 9–20.

Okechukwu, P. E., & Rao, M. A. (1996). Kinetics of cornstarch granule swelling in excess water. In P. A. Williams, G. O. Phillips, & D. J. Wedlock (Eds.), *Gums and stabilizers for the food industry-8* (pp. 49–57). Oxford: Oxford University Press.

Petridis, D. (1997). *Applied statistics for food technologists* (1st ed.., pp. 173–254). Thessaloniki: Homer Publishing (in Greek).

Raphaelides, S. N. (1986). *The nature of amylose-lipid interactions and their effect on the rheology of starch*. Ph.D. Thesis, University of Strathclyde, Glasgow.

Rodriguez, G., Vasseur, J., & Courtois, F. (1996). Design and control of drum dryers for the food industry, Part 1. Set-up of a moisture sensor and an inductive heater. *Journal of Food Engineering, 28*, 271–282.

Rosenthal, A., & Sgarbieri, V. C. (1992). Nutritional evaluation of a fresh sweet corn drum drying process. In A. S. Mujumdar (Ed.), *Drying '92* (pp. 1419–1425). Amsterdam: Elsevier.

Svenson, E., Gudmundsson, M., & Eliasson, A. (1996). Binding of Sodium dodecylsulphate to starch polysaccharides quantified by surface tension measurements. *Colloids and Surfaces B: Biointerfaces, 6*, 227–233.

Straub, J., Rosner, N., & Grigull, U. (1980). Oberflächenspannung von leichtem und schwerem wasser. *Wärme- und Stoffübertragung*, 241–252.

Straub, R. J., Tung, J. Y., Koegel, R. G., & Bruhn, H. D. (1979). Drum drying of plant juice protein concentrates. *Transactions of the ASAE, 22*(3), 484–486 (see also p. 493).

Trystram, G., & Vasseur, J. (1992). The modeling and simulation of a drum dryer. *International Chemical Engineering, 32*(4), 689–705.

Vallous., N. A., Gavrielidou, M. A., Karapantsios, T. D., & Kostoglou, M. (2001). Performance of a double drum dryer for producing pregelatinized maize starches. *Journal of Food Engineering* (accepted).

Vasseur, J., & Loncin, M. (1983). High heat transfer coefficient in thin film drying: Application to drum drying. In B. M. McKenna (Ed.), *Engineering and Food: Vol. 1. Engineering sciences in the food industry, Proceedings of 3rd International Congress, Dublin, Ireland* (pp. 217–225). Barking, Essex: Elsevier.

Vasseur, J., Abchir, F., & Trystram, G. (1991). Modelling of drum drying. In A. S. Mujumdar, & I. Filkova (Eds.), *Drying '91* (pp. 121–129). Amsterdam: Elsevier.

Wang, J. C. Y., Qiu, L. J., & Wang, S. F. (1990). Enhanced condensation inside a horizontal rotating drum-drier. *Drying Technology, 8*(4), 829–843.

Wong, R. B. K., & Lelievre, J. (1981). Viscoelastic behavior of wheat starch pastes. *Rheological Acta, 20*, 299–307.

Xu, Z., & Raphaelides, S. N. (1998). Flow behavior of concentrated starch dispersions using a tube rheometer of novel design. *Journal of Texture Studies, 29*, 1–13.

Ziegler, G. R., Thompson, D. B., & Casasnovas, J. (1993). Dynamic measurement of starch granule swelling during gelatinization. *Cereal Chemistry, 70*(3), 247–251.